

## Measuring high speed crack propagation in concrete fracture test using mechanoluminescent material

Wha-Jung Kim<sup>1</sup>, Jae-Min Lee<sup>1</sup>, Ji-Sik Kim<sup>2</sup> and Chang Joon Lee<sup>\*1</sup>

<sup>1</sup>School of Architecture and Civil Engineering, Kyungpook National University, Daegu, South Korea

<sup>2</sup>Department of Advanced Materials Engineering, Kyungpook National University, Sangju, South Korea

(Received February 17, 2012, Revised August 20, 2012, Accepted September 10, 2012)

**Abstract.** Measuring crack length in concrete fracture test is not a trivial problem due to high speed crack propagation. In this study, mechanoluminescent (ML) material, which emits visible light under stress condition, was employed to visualize crack propagation during concrete fracture test. Three-point bending test was conducted with a notched concrete beam specimen. The cracking images due to ML phenomenon were recorded by using a high speed camera as a function of time and external loadings. The experimental results successfully demonstrated the capability of ML material as a promising visualization tool for concrete crack propagation. In addition, an interesting cracking behavior of concrete bending fracture was observed in which the crack propagated fast while the load decreased slowly at early fracture stage.

**Keywords:** mechanoluminescence; concrete fracture; high speed crack detection; cracking images; three-point bending test

### 1. Introduction

Concrete is a quasi-brittle material which shows additional energy absorption capacity even after reaching its maximum strength. Due to the quasi-brittle characteristic, one can observe stable crack propagation in concrete fracture test using closed-loop testing system (Shah *et al.* 1995, Mier 1997). Closed-loop testing system usually employs crack-mouth-opening- displacement (CMOD) as a control signal for concrete fracture test. In order to provide stable crack propagation, the testing system controls hydraulic actuator so that the CMOD maintains a constant rate of increase. Once the stable crack propagation is obtained during the test, one can estimate crack length using traditional measuring tools such as optical travelling microscope, which can identify tiny crack tips of stationary posed cracks in quasi-brittle materials (Labuz *et al.* 1985).

It is generally understood that the use of controlled fracture test scheme is inevitable to obtain stable crack propagation, to measure crack length, and to quantify fracture properties. However the reality of concrete fracture is far away from the cracking behavior of controlled experiment. When applied load exceeds the maximum strength of concrete, cracks are initialized and propagate rapidly without any constraints. This cracking behavior is more similar to that of unmanipulated fracture test, which does not use any constraints for stable crack propagation after maximum load but let the specimen fail naturally. Therefore, in the viewpoint of phenomenological similarity, to study cracking

---

\*Corresponding author, Research Professor, E-mail: [cjlee0000@gmail.com](mailto:cjlee0000@gmail.com)

behavior of concrete in unmanipulated fracture test helps to understand more fundamental aspects of concrete fracture.

The testing equipment for unmanipulated fracture test is much simpler than that for controlled fracture test since no displacement control scheme is required. However, crack length measurement in unmanipulated fracture test is more complicated than that in controlled fracture test. The crack propagation in unmanipulated fracture test is not stable and very fast. Due to the high speed crack propagation, traditional measuring tools such as optical travelling microscope cannot be the option for crack length measurement.

Alternative method for crack length measurement in unmanipulated fracture test is to use surface strain gauges. In this method, strain gauges are installed near the crack path (not on the crack path) to measure strain changes in perpendicular direction to the crack path. During the crack propagation, the strain near the crack tip is abruptly changed and this strain change can be recorded as a function of time using high speed data logging system. Using the time and strain information, one can estimate the crack length as a function of time (Yu *et al.* 2010). Although this method is very useful to estimate crack length with fast loading rates and fast crack propagation, there are several limitations: the crack path should be known prior to the test; only small number of surface strain gauges can be installed to lab-size testing specimens hence the resolution of the crack length estimation is very limited.

A novel technology in material science, Mechanoluminescent (ML) material, has been focused and developed in the past decades due to its potential capability as a stress indicator (Xu *et al.* 1999, 2000, Sohn *et al.* 2002, Kim *et al.* 2003, 2005, Sohn *et al.* 2005, Kim *et al.* 2008, Li *et al.* 2008). The ML materials have similar aspects to piezoelectric materials such as *Pb-Zr-Ti*. Piezoelectric materials emit electric signal when mechanically excited (Giurgiutiu 2008). On the other hand, ML materials emit visible light when mechanically excited. The visible light emission under stress condition can be a powerful tool for monitoring crack propagation in fracture test.

Good examples of natural ML materials are sugar and quartz crystals. However, the ML efficiency of the materials is not enough for practical applications. Some efficient synthetic ML materials have been emerged (Xu *et al.* 1999, Kim *et al.* 2003, Sohn *et al.* 2005) and *SrAl<sub>2</sub>O<sub>4</sub>:Eu,Dy* phosphor is one of the promising synthetic ML materials. *SrAl<sub>2</sub>O<sub>4</sub>:Eu,Dy* phosphor has been used as a stress indicator since it was prepared in a bulky epoxy mixture form (Sohn *et al.* 2002). The researchers developed the “stress indicator” with *SrAl<sub>2</sub>O<sub>4</sub>:Eu,Dy* phosphors in various forms such as sintered ceramics (Kim *et al.* 2003), paints (Kim *et al.* 2005), and thin films (Sohn *et al.* 2005, Li *et al.* 2008).

This study investigated the capability of the ML material as a visualization tool for concrete crack propagation in unmanipulated fracture test. For this purpose a simple experimental program was designed. The experimental program conducted Mode I fracture test of a notched concrete beam using three-point bending configuration. A paint type ML material and a high speed camera were utilized to capture the images of high speed crack propagation under unmanipulated fracture condition.

## 2. Experiment

### 2.1 Fabrication of concrete specimen

A notched concrete beam specimen was prepared for the experiment. The specimen had dimensions of 50×100×400 mm and a notch of 50 mm as shown in Fig. 1. A normal strength concrete was used

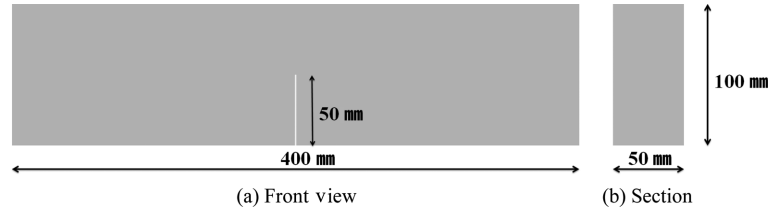


Fig. 1 Dimensions of notched concrete beam specimen

Table 1 Mixture proportion of concrete

Water (kg/m <sup>3</sup> )	Cement (kg/m <sup>3</sup> )	FA (kg/m <sup>3</sup> )	CA (kg/m <sup>3</sup> )
195.23	358.63	839.68	859.21

NOTE: FA=Fine Aggregate, CA=Coarse Aggregate

to fabricate the beam specimen. Table 1 shows the mixture proportion of the concrete material. The water-to-cement was 0.54 and the fine-to-coarse aggregates ratio was approximately 0.5. ASTM type I cement, crushed stone with maximum size of 10 mm and standard sand were used for the binder, coarse aggregates and fine aggregates, respectively.

The concrete mixing procedure was as follow. The fine aggregates and coarse aggregates were initially dry-mixed for 1 minute. Cement was added and dry-mixed for additional 1 minute. Water was added after dry-mixing procedure finished. The concrete was mixed for 5 additional minutes. All mixing procedure was conducted manually. After mixing, fresh concrete mixture was cast into a beam mold and 1 mm thick steel plate was inserted on the casting side in order to make a notch on the beam specimen. The specimen was cured in lab condition (25°C and 50% RH) for 12 hours. Subsequently it was de-molded and cured for 1 day in high temperature and humidity chamber (100°C and 100% RH) for fast strength gain.

## 2.2 Testing setup

Fig. 2 shows the experimental setup for three-point bending fracture test. A paint type ML material was prepared based on the work done by Kim *et al.* (2005), i.e., the ML paint was produced by mixing an epoxy resin with 15 vol.% of  $SrAl_2O_4:Eu,Dy$  powder. The ML paint was applied to 50 mm×50 mm area ahead of the notch tip. The ML paint applied on the specimen was cured for

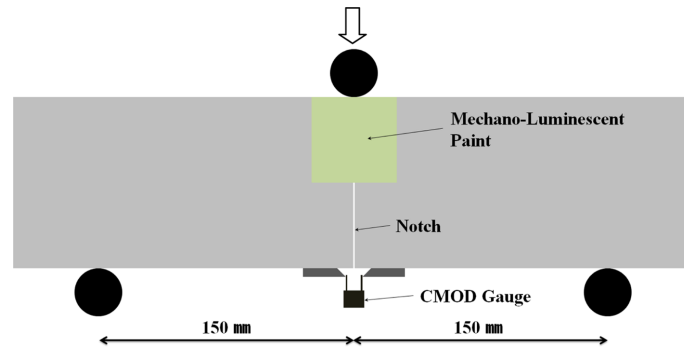


Fig. 2 Experimental setup for three-point bending fracture test

3 days in lab condition so that the epoxy resin could have enough stiffness. The thickness of the paint was approximately 0.2 mm.

A CMOD gauge was installed to the specimen with the help of knife edges attached near the notch mouth. The edge-to-edge space between the knife edges was 10 mm and the thickness of the knife edges was 6 mm.

### 2.3 Loading and data acquisition

The specimen was tested using three-point bending configuration. The span length between the lower supporting rollers was 300 mm. The ML paint on the specimen surface was excited by an ultraviolet lamp with wave length of 365 nm for 5 minutes prior to loading. A monotonic load was applied to the center of the beam specimen with the rate of 2 kN/min.

The visual images of the painted area were recorded using a high speed camera with the rate of 250 frame/sec. The loading signal was fed into the high speed camera system for the synchronization between the load and the cracking images. The load and CMOD signals were also recorded using a high speed data logging system with the rate of 250 sample/sec.

## 3. Results

### 3.1 Load-CMOD response and cracking images

Fig. 3 shows the load-CMOD response of the bending fracture test. The load-CMOD curve rapidly increases up to the maximum load of 1.5 kN and gradually decreases after that. It should be noted that the bending test was conducted using unmanipulated fracture test scheme; consequently the

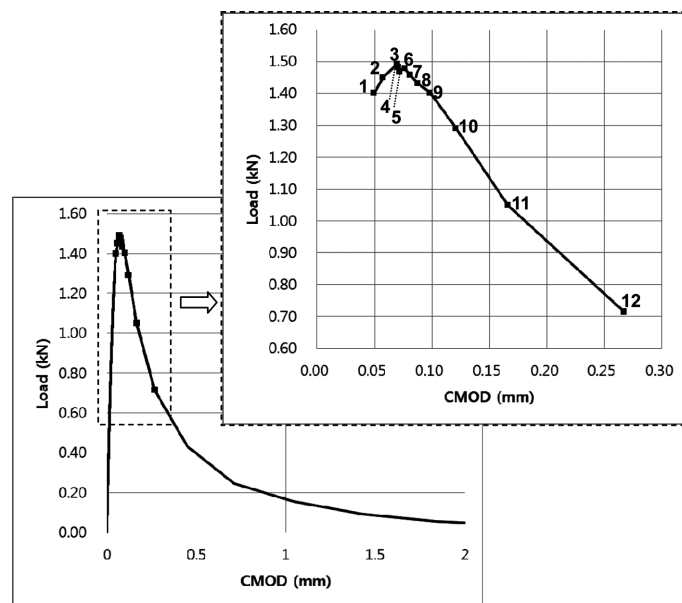


Fig. 3 Load-CMOD response

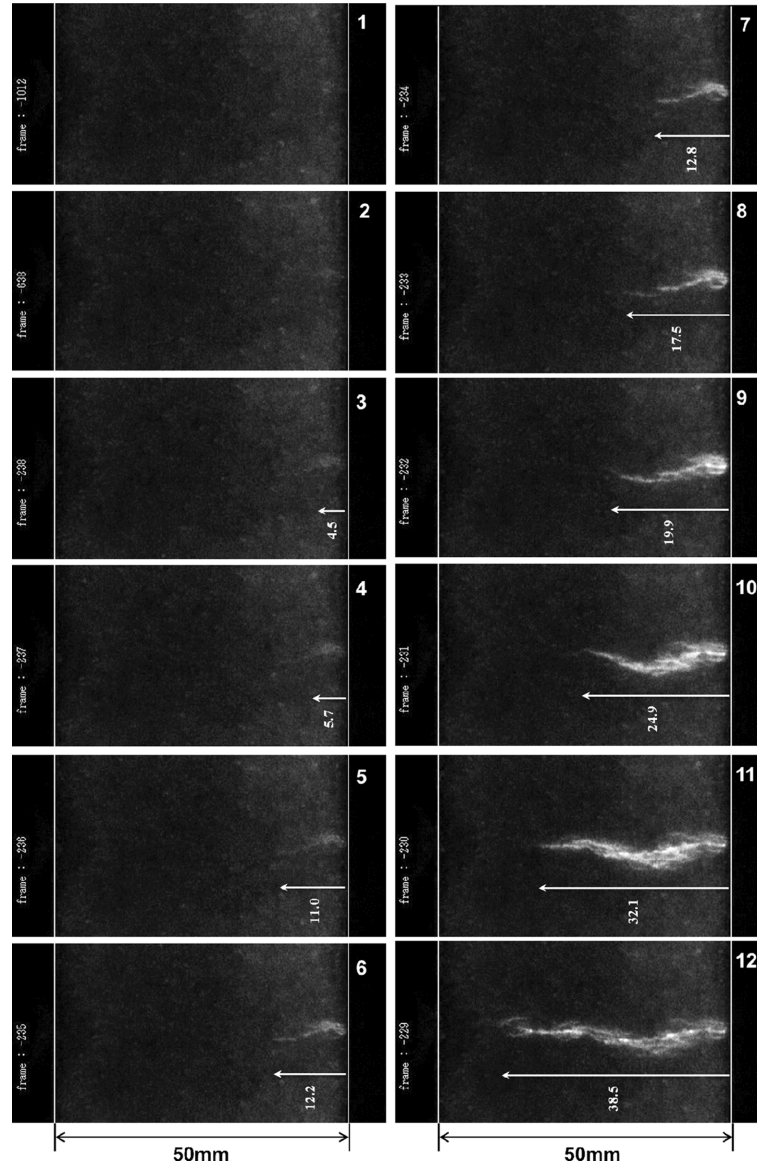


Fig. 4 Sequential ML images of crack propagation

load-CMOD response after maximum load was the result of natural failure of the beam specimen.

Fig. 4 shows the sequential images of the crack propagation. Each image in the figure represents the cracking status at the corresponding data point on the load-CMOD curve in Fig. 3. Images #1 - #3 belong to the loading region and the time gaps among the images are approximately 1.5 sec each. Images #3 - #12 belong to the natural failure region and the time gaps among the images are approximately 0.004 sec each. Images #1 and #2 show micro-crack initiation although they are not very clear due to the background noise of the images. The crack formation is much clear in Image #3, which corresponds to the peak location on the load-CMOD curve in Fig. 3. The crack propagation is clearly observed in Images #4 - #12.

3.2 Load, CMOD, and crack length change as a function of time

Figs. 5, 6, and 7 show the load, CMOD, and crack length changes as a function of time, respectively. The origin of time-axis in the figures corresponds to the time of maximum load of the fracture test. The load and CMOD information were obtained directly from the data logging system while the crack length was manually measured from the sequential images in Fig. 4.

The load change as a function of time (Fig. 5) shows a high nonlinearity with a turning point at the time of 0.024 sec. The load is slightly decreasing up to the time of 0.024 sec, subsequently it shows a rapid decrease. The CMOD change as a function of time (Fig. 6) shows a similar trend to the load change except for the changing direction. The CMOD is slightly increasing up to the time of 0.024 sec, subsequently it shows a rapid increase. The crack length change as a function of time

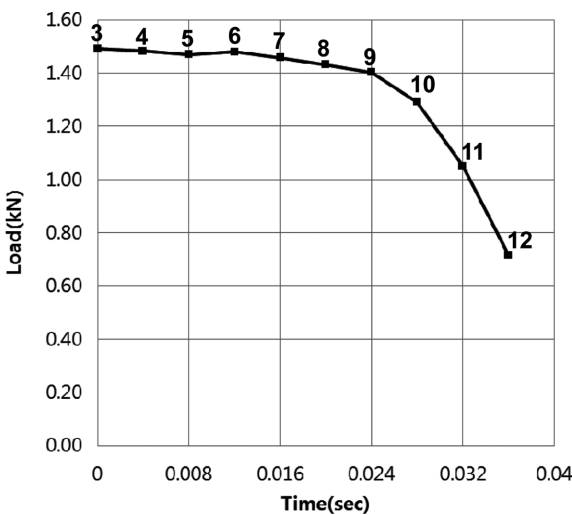


Fig. 5 Load change as a function of time

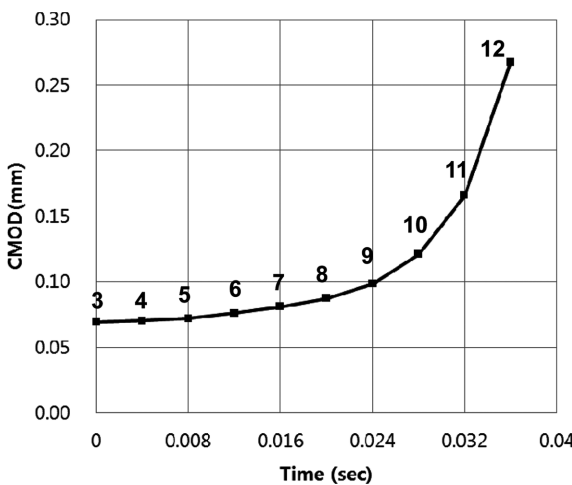


Fig. 6 CMOD change as a function of time

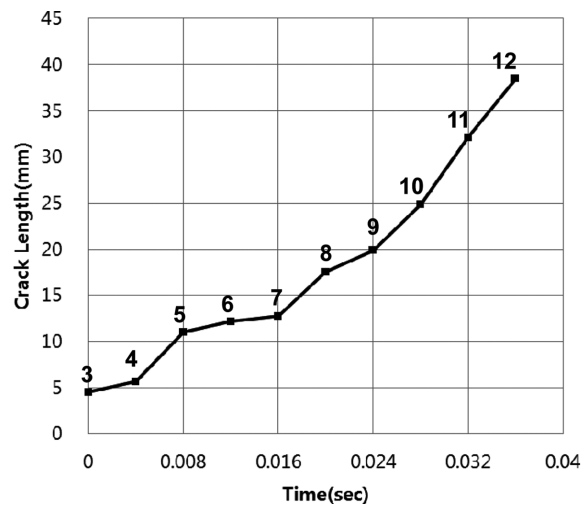


Fig. 7 Crack length change as a function of time

(Fig. 7) is quite different from the load and CMOD changes. The crack length increases in linear manner with no distinct turning point, which is observed in the load-time and CMOD-time curves at the time of 0.024 sec.

#### 4. Discussion

The original goal of this study is to investigate the capability of the ML material as a visualization tool for crack propagation in concrete fracture test. In this sense, the sequential crack images shown in Fig. 4 validate the achievement of the original goal. In addition to these images, several results of interest have been observed due to the unique feature of ML material, visible light emission under

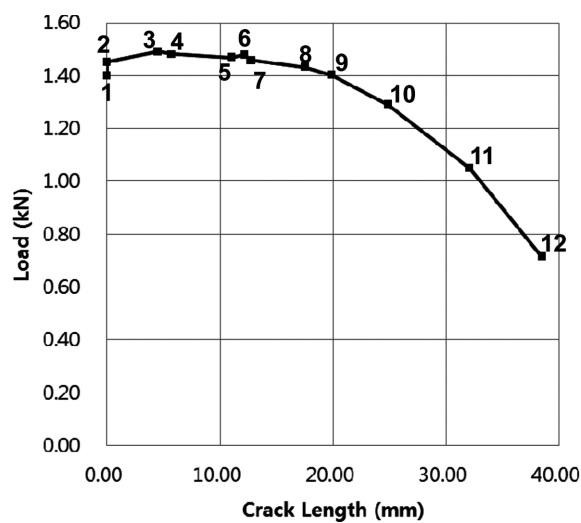


Fig. 8 Load vs. Crack length

stress condition.

Fig. 8 shows the load-crack length response of the test. The first insight regarding the crack propagation judged from the load-crack length curve is that the crack propagation at early fracture stage is quite fast compared to the load decrease. For instance, at the data point #9, the crack length is about 20 mm and the load is about 1.4 kN. The crack length of 20 mm is 40% of the maximum potential crack length (50 mm) of this test setup while the load of 1.4 kN is less than 10% decrease from the maximum load (1.5 kN).

The fast crack propagation at early fracture stage implies that the crack length increases continuously while the load is sustaining for a certain time period. The load as a function of time (Fig. 5) is almost sustaining up to the time mark of 0.024 sec. During this time period the crack length as a function of time (Fig. 7) is linearly increasing. This time period is defined here as “load sustaining period” of unmanipulated fracture test since it cannot be observed in displacement controlled fracture test.

The fast crack propagation during the load sustaining period is an interesting observation since it seems to be linked with the cross sectional cracking profile in concrete beam fracture. It was reported that, in controlled fracture test of concrete beam specimen, the crack length on the beam surface is greater than that in the interior beam. In other words, the cross sectional cracking profile along the crack path shows a saddle shape so that the crack front is shallow in the interior and deep on the beam surface.

The cross sectional profile in concrete beam fracture has been revealed by dye penetration technique (Swartz and Go 1984) and also acoustic emission technique (Maji *et al.* 1990). If we assume this cross sectional cracking profile for the unmanipulated fracture test, the fast crack propagation during the load sustaining period may be explained as: during the load sustaining period, very small amount of the overall cracked area was increased hence the resisting load was slightly decreased. However, during the same period, the surface crack propagated continuously so as to form the saddle shape of cross-sectional cracking profile.

## 5. Conclusions

This study employed ML paint to visualize fast crack propagation in concrete fracture test and successfully demonstrated the capability of ML paint as a promising visualization tool for high speed crack propagation. The experimental results also revealed that, in unmanipulated concrete fracture test, the surface crack propagation at early fracture stage is quite fast compared to the load decrease. The amount of load decrease at the early fracture stage was quite small compared to the magnitude of the maximum load. Based on this fact, the early fracture stage was defined as “load sustaining period” in unmanipulated concrete fracture test. The reason for the fast surface crack propagation with slow load decrease was conjectured from the saddle shape of cross-sectional cracking profile of concrete beam which is usually observed in controlled bending fracture test.

## Acknowledgements

This research was supported by a grant (11-High-Tech-Urban-C02) from High-Tech Urban Development Program funded by Ministry of Land, Transport and Maritime Affairs of Korean



government. This research was also supported by Basic Science Research Program through the National Research Foundation of Korea Funded by the Ministry of Education, Science and Technology (2012-0001380).

## References

- Giurgiutiu, V. (2008), *Structural Health Monitoring with Piezoelectric Wafer Active Sensors*, Academic Press, Burlington, MA.
- Kim, J.S., Kwon, Y. and Sohn, K. (2003), "Dynamic visualization of crack propagation and bridging stress using the mechano-luminescence of  $\text{SrAl}_2\text{O}_4$ : (Eu, Dy, Nd)", *Acta Mater.*, **51**(20), 6437-6442.
- Kim, J.S., Kwon, Y., Shin, N. and Sohn, K. (2005), "Visualization of fractures in alumina ceramics by mechanoluminescence", *Acta Mater.*, **53**(16), 4337-4343.
- Kim, J.S., Koh, H.J., Lee, W.D., Shin, N., Kim, J.G., Lee, K.H. and Sohn, K.S. (2008), "Quasi-dynamic visualization of crack propagation and wake evolution in Y-TZP ceramic by mechano-luminescence", *Met. Mater. Int.*, **14**(2), 165-169.
- Li, C., Xu, C.N., Zhang, L., Yamada, H. and Imai, Y. (2008), "Dynamic visualization of stress distribution on metal by mechanoluminescence images", *J. Visual.*, **11**(4), 329-335.
- Maji, A.K., Ouyang, C. and Shah, S.P. (1990), "Fracture mechanism of quasi-brittle materials based on acoustic emission", *J. Eng. Mech.- ASCE*, **5**(1), 206-217.
- Mier, J.G.M. (1997), *Fracture Processes of Concrete*, CRC Press Inc, Boca Raton, FL.
- Shah, S.P., Swartz, S.E. and Ouyang, C. (1995), *Fracture mechanics of concrete: applications of fracture mechanics to concrete, rock and other quasi-brittle materials*, John Wiley & Sons Inc., New York, NY.
- Sohn, K.S., Seo, S.Y., Kwon, Y.N. and Park, H.D. (2002), "Direct observation of crack tip stress field using the mechanoluminescence of  $\text{SrAl}_2\text{O}_4$ : (Eu, Dy, Nd)", *J. Am. Ceram. Soc.*, **85**(3), 712-714.
- Sohn, K.S., Park, D.H. and Kim, J.S. (2005), "Luminescence of pulsed-laser deposited  $\text{SrAl}_2\text{O}_4$ : Eu, Dy thin film and its role as a stress indicator", *J. Electrochem. Soc.*, **152**(10), 161-167.
- Swartz, S.E. and Go, C.G. (1984), "Validity of compliance calibration to cracked concrete beams in bending", *Exp. Mech.*, **24**(2), 129-134.
- Xu, C.N., Watanabe, T., Akiyama, M. and Zheng, X.G. (1999), "Direct view of stress distribution in solid by mechanoluminescence", *Appl. Phys. Lett.*, **74**(17), 2414-2416.
- Xu, C.N., Zheng, X.G., Akiyama, M., Nonaka, K. and Watanabe, T. (2000), "Dynamic visualization of stress distribution by mechanoluminescence image", *Appl. Phys. Lett.*, **76**(2), 179-181.
- Labuz, J.F., Shah, S.P. and Dowding, C.H. (1985), "Experimental analysis of crack propagation in granite", *Int. J. Rock Mech. Min.*, **22**(2), 85-98.
- Yu, R.C., Zhang, X.X., Ruiz, G., Tarifa, M. and Cámara, M. (2010), "Size of the fracture process zone in highstrength concrete at a wide range of loading rates", *Appl. Mech. Mater.*, **24-25**, 155-160.